Predicting Human Control Adaptation from Statistical Variations in Tracking Error and Error Rate

van Ham, Jacomijn M.; Pool, Daan M.; Mulder, Max

DOI
10.1016/j.ifacol.2022.10.250

Publication date
2022

Document Version
Final published version

Published in
IFAC-PapersOnline

Available online at www.sciencedirect.com

ScienceDirect

IFAC Papers Online CONFERENCE PAPER ARCHIVE

IFAC PapersOnLine 55-29 (2022) 166–171

Predicting Human Control Adaptation from Statistical Variations in Tracking Error and Error Rate

Jacomijn M. van Ham,* Daan M. Pool,* and Max Mulder*

* *Control and Simulation Section, Aerospace Engineering, Delft University of Technology, Delft, The Netherlands (e-mail: {d.m.pool, m.mulder}@tudelft.nl).*

Abstract: This paper presents the results of an experiment that was performed to verify the '*supervisory control algorithm*', a well-known model of human operator adaptation to changes in controlled element dynamics. This model proposes that human adaptive behavior is triggered once the magnitudes of the tracking error or error rate exceed certain decision region limits. In the experiment, a compensatory tracking task with a sudden transition in the controlled element dynamics, as also tested in other recent experiments, was performed by six skilled participants. In addition to performing the control task, participants had to indicate with a button press when they detected a controlled element transition. The results indicate that the published detection limits for the 'supervisory control algorithm' are too conservative for our experiment data, as measured detections could be related to error or error rate occurrences that exceeded 2-6 times their respective pre-transition standard deviations. The effectiveness of new detection limits proportional to these pre-transition standard deviations was tested. The best match to our experiment data was obtained with limits at 3.9σ, for which in only 9.38% and 11.5% of cases a (false positive) too early detection or a (false negative) missed detection occurred, respectively. Overall, these results demonstrate that human operator adaptation can indeed be effectively predicted from statistical variations in tracking error and error rate.

Keywords: Cybernetics, manual control, human operator adaptation, time-varying behavior

1. INTRODUCTION

In this era of increasing automation, in which for many applications human controllers are increasingly removed from the control loop, human controllers' ability for 'fast' adaptations to changes in task dynamics remains an essential source of inspiration for adaptive automation design (Phatak, 1969; Mulder et al., 2018). Humans are still unsurpassed when it comes the effectiveness of their control adaptations, which are generally fully realized in 2-5 seconds depending on the type of transition (Young et al., 1964). Of special recent interest are human control adaptations to sudden changes in the dynamics of the system that is controlled, i.e., the Controlled Element (CE) (Hess, 2009; Zaal, 2016; Mulder et al., 2018; Plaetinck et al., 2019).

Young et al. (1964) identified three main phases of the human control adaptation process: 1) *detection*, where the human operator detects a change in CE dynamics; 2) *identification*, where the human operator correctly identifies the new CE dynamics; 3) *modification*, where operators adapt their own control dynamics to the new CE. The key driver of this adaptation process is believed to be an '*internal model*' of their task that human operators build up and that enables them to notice when, for example, the characteristics of occurring control errors (e) and error rates ($\dot{e}$) change (Miller and Elkind, 1967; Phatak and Bekey, 1969b; Niemela and Krendel, 1975; Hess, 2009; Weir and Phatak, 1967; Mulder et al., 2018). This hypothesis for modeling the human adaptive process is formalized in the '*supervisory control algorithm*' (Phatak and Bekey, 1969b,a; Phatak, 1969), which defines explicit limits on tracking error and error rate that trigger human operators to detect, identify, and adapt to a change in CE dynamics. However, at present the detection limits proposed in this adaptive human control framework have not been validated, nor has the model been compared to recent experiment data on human control adaptation (Zaal, 2016; Plaetinck et al., 2019).

The goal of this paper is to verify whether human controllers' detection of changes in CE dynamics can be predicted based on outliers that occur in tracking error and error rate compared to their expected statistical variations. To achieve this goal, an experiment was run with six trained participants who performed a compensatory pitch tracking task with time-varying CE dynamics, as also considered in several earlier experiments (Plaetinck et al., 2019; Zaal, 2016). Participants were instructed to focus on detecting CE dynamics changes while performing the tracking task and to report these subjective detections by pressing a button on the front of their side stick. The results of this experiment were used to verify if human controllers' detections could be predicted from deviations in the statistical properties of the error and error rate in a human adaptive control framework as proposed by Phatak and Bekey (1969b).

10.1016/j.ifacol.2022.10.250

2. BACKGROUND

The model considered for the prediction of adaptive human control in this research is the '*supervisory control algorithm*' (Phatak and Bekey, 1969b,a; Phatak, 1969). Fig. 1 shows the structure of this model, implemented in the block scheme of a compensatory tracking task. In such a task, human operators aim to minimize the tracking error e, thereby making the CE's output y follow the target signal f_t. The 'Supervisor' and 'Human Operator Dynamics' blocks together represent the model of the adaptive human controller. The 'Supervisor' is a higher-level controller that implements a four-phase decision-making process assumed to occur in human control adaptation (Phatak, 1969): 1) *pre-transition retention* (i.e., controlling the post-transition CE dynamics, assuming the pre-transition dynamics), 2) *detection of the change*, 3) *identification of the new CE dynamics*, and 4) *post-transition steady-state tracking*. The 'Supervisor' then drives the adaptation by reorganizing the structure of the 'Human Operator Dynamics' based on an internal model of different potential CE dynamics. As shown in Fig. 1, the main input to the 'Supervisor' is the tracking error signal e. The control input u is also an hypothesized input for detecting a CE change (Phatak, 1969), however, its potential contribution has so far not been investigated.

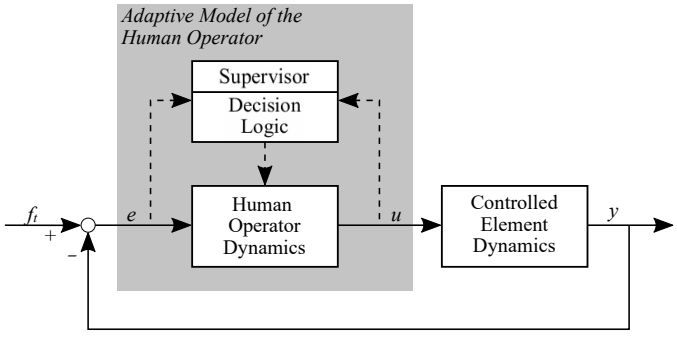

Fig. 1. Hypothetical structure of the adaptive human operator model (Phatak, 1969).

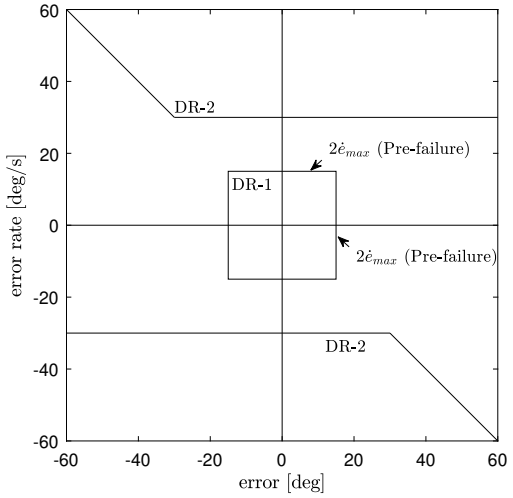

Fig. 2. Proposed decision regions of the Supervisor's sequential identification (Phatak and Bekey, 1969b).

The 'Supervisor' algorithm is based on sequential 'yes' or 'no' decisions by following the development of the error and error rate during a run, induced by a sudden transition in CE dynamics. These decisions determine when and how the human operator will adapt her control strategy to maintain stable control. The algorithm's decisions are based on the instantaneous magnitudes of error (e) and error rate ($\dot{e}$), as well as sign changes of the error rate. Fig. 2 displays a phase plane (e on the x-axis and $\dot{e}$ on the y-axis) with the decision regions (DRs) as defined by (Phatak, 1969). These decision regions define the moment of a binary decision by the supervisory control algorithm, as well as the type of action taken.

The DR limits shown in Fig. 2 were determined by analyzing data of experimentally measured transitions (Phatak and Bekey, 1969b). The exact values of e and $\dot{e}$ where the DR limits occur are part of the 'internal model' operators develop by performing the task: they are based on past information of the (pre-transition) system. In this paper, we will focus on the first decision region, DR-1 in Fig. 2, which represents the limits beyond which human operators are hypothesized to detect a change in CE dynamics. As can be verified from Fig. 2, Phatak and Bekey (1969b) defined the DR-1 limits for both e and $\dot{e}$ to be at $2\dot{e}_{max}$, where $\dot{e}_{max}$ is the maximum (absolute) occurring peak in steady-state (pre-transition) error rate.

3. METHOD

3.1 Control Task

The human-in-the-loop experiment was similar to earlier experiments on time-varying human operator behavior (Zaal, 2016; Plaetinck et al., 2019). Participants were asked to perform a compensatory pitch attitude tracking task, in which the tracking error e (f_t-y, see Fig. 1) was presented using a simplified primary flight display, see Fig. 3(a). Participants tracked a quasi-random sum-of-sinusoids target signal (f_t) consisting of 10 sines with a measurement window of 90 s. The CE dynamics were defined using a second-order transfer function (Zaal, 2016) $H_c(s,t) = K_c(t)/(s(s+\omega_b(t)))$, where the CE gain K_c and break frequency ω_b were both time-varying. To simulate a transition from approximately single integrator (SI) to double integrator (DI) CE dynamics (Zaal, 2016), both parameters were varied according to a sigmoid function (K_c: 90 to 30, ω_b: 6 to 0.2 rad/s) with a maximum rate of change (G in the notation of Zaal (2016)) of 100 s^{-1}. The sigmoid's moment of maximum rate of change (M) was varied across different tested cases, see Section 3.4.

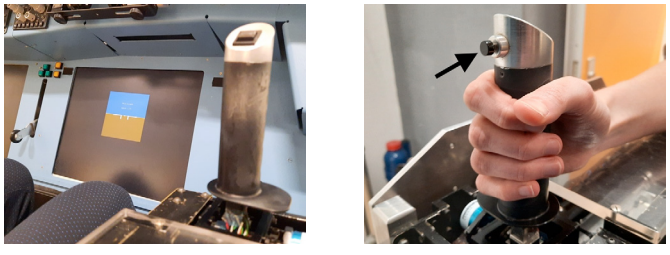

(a) Simulator set-up (b) Button on the side stick

Fig. 3. Fixed-base simulator experiment set-up.

Table 1. Experiment conditions

Condition	f_t	M [s]	Condition	f_t	M [s]
C1	1	33.5	C2	1	42.5
C3	2	37.5	C4	2	38.5
C5	3	35.5	C6	3	36.5
C7	4	44.0	C8	4	33.0
C9	5	42.0	C10	5	36.5
C11	6	42.5	C12	6	41.0
C13	7	41.0	C14	7	44.5
C15	8	33.5	C16	8	36.5

3.2 Apparatus

The experiment was performed in the *Human-Machine Interaction Laboratory* at TU Delft, a fixed-based simulator with a right-handed side stick, see Fig. 3(a). The stick moved up to ±22 deg in forward/backward direction only and its spring constant, inertia, damping constant and break-out moment were set to 5.0 Nm/rad, 0.01 kg/m^2, 0.2 Nm s/rad and 0.0 Nm, respectively. Participants used the trigger button on the front of the side stick, see Fig. 3(b), to provide a subjective detection of a CE change.

3.3 Participants and Instructions

The experiment was approved by the Human Research Ethics Committee (HREC) of TU Delft (application number 1,352). Six participants performed the experiment; all were MSc students at TU Delft and between 20 and 30 years old. All had prior experience with tracking tasks from earlier experiments. They were briefed on the experiment procedures, the control task, and the simulator setup. The instruction was to track as accurately as possible, while also paying attention to potential changes in the CE dynamics. When they detected a change, they were instructed to press the button on the front of the side stick, see Fig. 3(b). After each run, the participants' tracking score (rms of e) was shown; they did not receive any feedback about their performance in detecting the transition.

3.4 Experiment Conditions

As listed in Table 1, the experiment collected human control data for a total of 16 experiment conditions, defined by a combination of levels of the following two variables: the target signal realization and the moment of occurrence of the CE transition. To prevent participants from memorizing and anticipating the target signal, eight different f_t realizations with different sinusoid phase shifts $\phi_t[n]$ were used, see Table 2. The sine frequencies $\omega_t[n]$ and amplitudes $A_t[n]$ were identical for the different f_t realizations. Furthermore, to avoid artifacts due to participants' anticipation of the CE transition, two different transition times (sigmoid parameter M) were defined for each f_t realization, see Table 1.

3.5 Experiment Procedure

The total tracking run length was 95 s, including 5 s of run-in time. As shown in Fig. 4, the remaining 90 s of measurement time was split over three separate 30-second windows. The target signal f_t was designed to have a period of 30 s, thus exactly the same signal was tracked

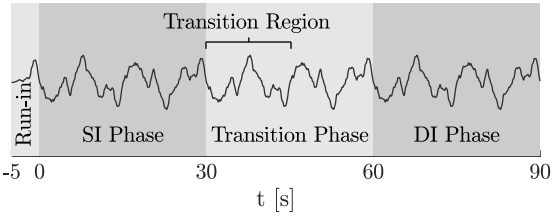

Fig. 4. Example of a run with its periodic target signal, showing the different phases and the transition region.

across the three windows to facilitate direct comparison. During the first 30-second period participants tracked the SI CE dynamics. Then, at a variable moment in the 'Transition Region' (see M in Table 1) the CE dynamics changed to approximate a DI. Within the 'Transition Phase' the participants had to detect the CE change and adapt their response to continue stable tracking. During the last 30-second phase participants performed steady-state tracking of the post-transition DI dynamics.

In the experiment, data from a total of 16 runs (one for each condition) were collected from each participant. These 16 measurement runs were performed in a randomized order across the different participants to eliminate order effects. Note that a perfectly balanced design was not possible with our six participants. Prior to the measurement runs, all participants were trained for 3-5 runs with time-invariant CE dynamics for both SI and DI, as well as 3-5 runs including the CE transition, until they showed constant performance. Finally, 3-5 runs with the time-varying CE were performed to practice with the subjective detection and button press. The full experiment was completed in approximately 1 hour per participant.

3.6 Data Analysis

Our analysis focused on determining the "outlying" post-transition e or $\dot{e}$ occurrences that caused the participants to detect a change, see Fig. 5. Between participants' detection of a CE change and the recorded button, some Reaction Time (RT) is expected. Based on research by Thorpe et al. (1996), who measured reaction times for button presses in response to visual inputs, the minimum and maximum RT values expected for our data were 0.3 s

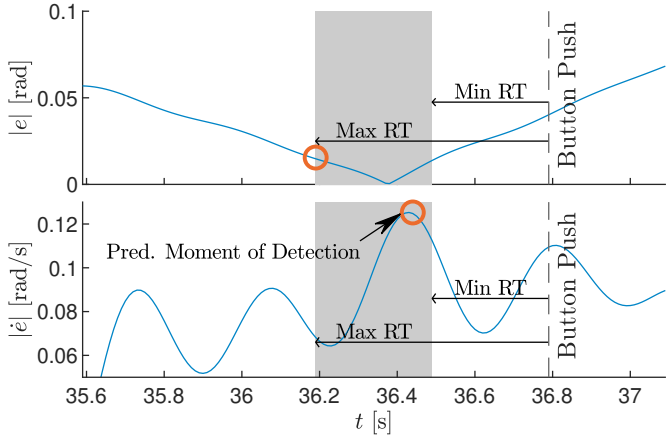

Fig. 5. Predicted moment of detection determined by error rate for an example run.

Table 2. Forcing functions parameter values

$k_t[-]$	$\omega_t[rad/s]$	$A_t[deg]$	$\phi_{t,1}[rad]$	$\phi_{t,2}[rad]$	$\phi_{t,3}[rad]$	$\phi_{t,4}[rad]$	$\phi_{t,5}[rad]$	$\phi_{t,6}[rad]$	$\phi_{t,7}[rad]$	$\phi_{t,8}[rad]$
3	0.63	0.888	3.01	3.61	4.20	3.55	1.00	0.90	2.31	0.78
7	1.47	0.481	2.33	5.06	2.26	4.29	5.21	1.51	6.05	4.73
11	2.30	0.269	3.84	0.27	1.29	0.48	4.84	2.59	0.52	0.95
17	3.56	0.138	4.29	2.83	3.83	4.31	1.33	4.67	2.98	1.37
21	4.40	0.103	5.51	2.93	0.40	3.10	4.23	3.70	5.74	1.05
29	6.07	0.063	3.71	3.06	3.33	3.56	5.52	6.14	6.08	2.30
41	8.59	0.040	0.94	3.32	0.55	5.94	2.05	0.01	4.85	1.03
53	11.10	0.034	5.77	6.04	2.09	1.18	5.43	2.23	4.17	2.95
71	14.97	0.034	4.29	0.32	0.08	1.49	4.36	6.24	6.02	2.70
87	18.22	0.023	2.31	1.62	0.43	4.70	0.71	5.40	3.66	5.89

and 0.6 s, respectively. As shown in Fig. 5, the predicted moment of detection was determined by 1) finding the highest peaks in e or $\dot{e}$ in the gray-shaded window, 2) normalizing the peak values with their respective steady-state standard deviations in the pre-transition SI tracking phase, and 3) selecting the most "outlying" e or $\dot{e}$ value as the likely trigger for the participant to detect the transition (Young, 1969). Fig. 5 shows an example where the predicted detection is attributed to an $\dot{e}$ peak.

4. RESULTS

4.1 Detection Lag

In total 96 tracking runs were performed across all six participants. The detection lag, calculated as the time difference between the CE change (M) and a participant's button push, is shown per condition in Fig. 6. Colored lines show the detection lag for each participant (P1-P6) per condition. Boxplots indicate the variation across all participants for each condition. The median of all measured detection lags was found to be 6.6 s, the horizontal dashed red line in Fig. 6; this is consistent with the earlier experiment of Plaetinck et al. (2019), who found lags between 2.2 s and 7.4 s. Fig. 6 further shows that there were three false positive detections (for P3 and P6 only), i.e., moments where participants pressed the button *before* a transition, and one false negative (for P4), where the transition was not detected.

Furthermore, Fig. 6 shows that participants consistently detected a CE change more quickly for specific conditions (e.g., condition 12) and took consistently longer for others (e.g., condition 8). This indicates that, as expected, the forcing function characteristics at the moment of transition (and hence the f_t realization) impact how long it takes for participants to detect a CE transition. While our current 16 conditions are insufficient to fully characterise this dependency, this result shows that this is a key factor that may affect experiments with time-varying CE dynamics and should be accounted for when designing experiments.

4.2 Detection Error and Error Rate Analysis

The DR-1 decision region from (Phatak and Bekey, 1969b), shown in Fig. 2, is intended to encompass error and error rate magnitudes representative for pre-transition tracking. In this paper, the pre-transition tracking was always performed with the same CE dynamics, which closely resemble a single integrator in the crossover region,

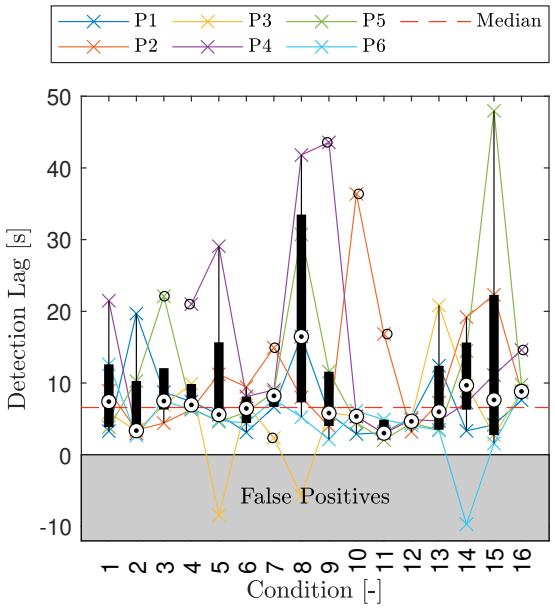

Fig. 6. Detection lag per experiment condition.

see Section 3.1. Fig. 7 shows the measured range of all pre-transition e and $\dot{e}$ values as the blue surface, which is a top view on the 2-dimensional distribution of all measured error and error rate values. The outlying post-transition e or $\dot{e}$ values that were linked to the subjective button press data, see Section 3.6, are plotted with red cross symbols. The three false positives (see Fig. 6) are indicated with yellow crosses. The diagonal lines in Fig. 7 separate the detections based on e or $\dot{e}$ outliers, see Section 3.6; detections in the left and right quadrants (41 out of 95) are due to peaks in e, while those in the top and bottom quadrants (54 out of 95) are linked to outlying $\dot{e}$ values.

Fig. 7 further shows the DR-1 limits from (Phatak and Bekey, 1969b), here calculated from the average maximum $\dot{e}$ across all participants, using a black dash-dotted line. Comparison with our detection data (cross markers) shows that only one of the detections in fact corresponds to an e or $\dot{e}$ value outside the DR-1 region, i.e., 95.8% lie within the previously proposed DR-1 region. Furthermore, Fig. 7 shows that the e or $\dot{e}$ values that led to detections are at the outskirts of the natural variation in e or $\dot{e}$ during SI tracking (blue area), which contrasts with the square shape of the DR-1 limits. The dashed and dotted lines indicate the regions of 2σ and 6σ, respectively, with respect to the

Table 3. Individual and average pre-transition e and $\dot{e}$ standard deviations and DR-1 limits.

	P1	P2	P3	P4	P5	P6	Mean
σ_e [rad]	0.023	0.022	0.023	0.023	0.024	0.022	0.023
$\sigma_{\dot{e}}$ [rad/s]	0.047	0.043	0.046	0.042	0.046	0.043	0.045
$2\lvert\dot{e}_{max}\rvert$ [rad/s]	0.312	0.291	0.276	0.255	0.299	0.253	0.281

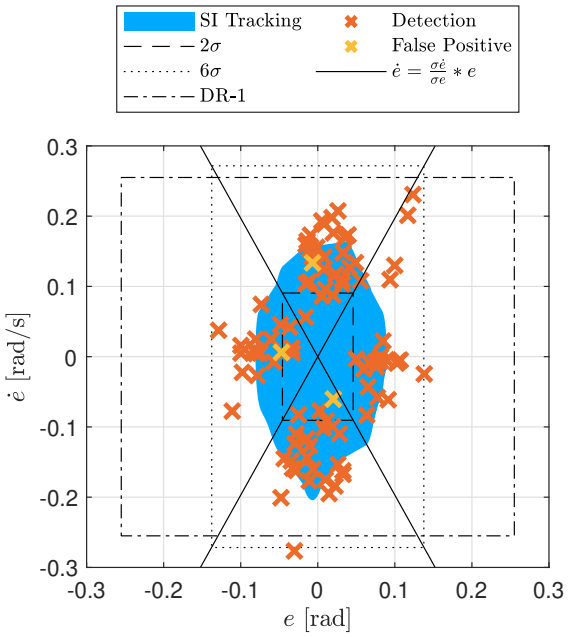

Fig. 7. Spread in pre-transition tracking errors and error rates compared to measured detections.

mean of the pre-transition SI tracking data. Especially the 2σ-region, which assuming a normal distribution encloses around 95% of the pre-transition e and $\dot{e}$ data, includes only 8.4% of the measured detections, as well as one of the false positives. This suggests that detection limits for predicting human adaptation based on the statistical variations that occur in pre-transition error and error rate signals may be more effective than the DR-1 limits.

Table 3 presents the pre-transition standard deviations for error and error rate – σ_e and $\sigma_{\dot{e}}$, respectively – for each participant, as well as the corresponding DR-1 limit values, $2\dot{e}_{max}$. The rightmost column lists the averages across all participants. Table 3 shows remarkable consistency in σ_e and $\sigma_{\dot{e}}$ across participants, with individual values that deviate less than 5% from the averages of 0.023 rad and 0.045 rad/s, respectively. Consistent with Fig. 7, Table 3 further indicates the unrealistically large gap – i.e., $2e_{max} \approx 12\sigma_e$ and $2\dot{e}_{max} \approx 6\sigma_{\dot{e}}$ – between normal pre-transition statistical variations in e and $\dot{e}$ and the DR-1 detection limit as proposed by Phatak and Bekey (1969b).

4.3 Proposed Detection Limits

Based on Fig. 7, we propose to base the detection limits that could be used to predict human operator adaptation on multiples of the pre-transition e and $\dot{e}$ standard deviations. As shown in Fig. 7, with a common factor on σ_e and $\sigma_{\dot{e}}$ this results in a 'rectangular' detection limit boundary. To determine this optimal factor for our experiment data, we considered the range of 2σ to 6σ and used our proposed new limits to determine the *first moment* at which either e or $\dot{e}$ passes this limit for each participant, i.e., we determined the predicted detection from the measured e and $\dot{e}$ data. For this analysis, we used the average standard deviations of the error and error rate as listed in Table 3. We also performed the same analysis with individual standard deviation limits for each participant, but given the consistency between participants (see Table 3), the results are equivalent and not presented here.

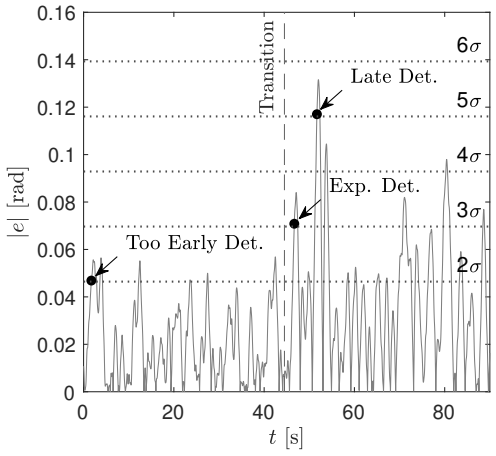

Fig. 8. Example absolute error signal showing the early, expected, and late detections that may occur for different detection limit values.

Fig. 8 shows an example (absolute) e signal from our experiment data, together with different e-detection limits (dotted horizontal lines) to illustrate our methodology. As shown in Fig. 8 for a detection limit of 3σ, *Expected detections* are detections that fall within range of the expected detection times, i.e., between 2.2-7.4 s after the CE transition (Plaetinck et al., 2019). Predicted detections that occur earlier than this, as would happen here for a 2σ limit, are labelled as *Too Early detections*, i.e., false positives. Detections that occur later than 7.4 s, see Fig. 8, are classified as *Late detections*. The final category of *No Detection* (not shown in Fig. 8) consists of all cases where no detection limit was crossed, i.e., false negatives. Note that while Fig. 8 only shows e, we in fact performed this analysis on both e and $\dot{e}$ and always used the first predicted detection based on either signal.

Fig. 9 shows the classification of predicted detections across all participants, using the average e and $\dot{e}$ standard deviations from Table 3 – i.e., 0.023 rad and 0.045 rad/s, respectively – as the reference pre-transition variability. The cumulative occurrence of Too Early, Expected, Late and No detections, which always adds up to 100%, is shown as a function of the detection limit magnitude. Fig. 9 shows that a limit below 2.5σ results in only Early detections. This is expected, as a single e or $\dot{e}$ occurrence that far from their respective means is highly likely, see also Fig. 8. At

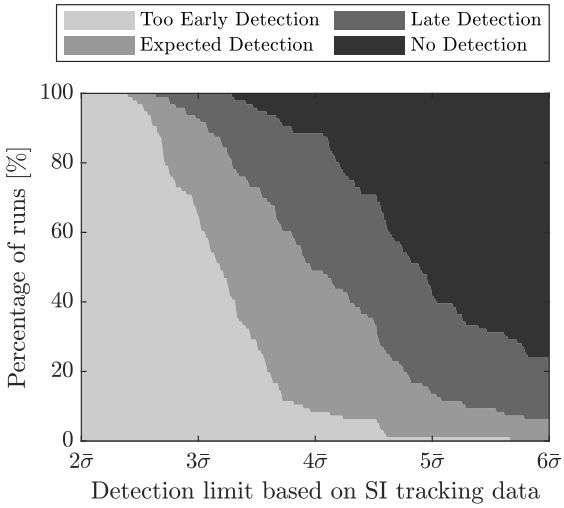

Fig. 9. Classification of predicted detections from the experiment data using average e and $\dot{e}$ standard deviations to define the detection limits.

around 4σ, mostly Expected and Late detections occur, meaning that false positives and false negatives are both mostly suppressed. For limit values above 4σ, cases with No detections quickly become dominant.

The detection limit with the lowest proportion of Too Early detections (9.38%) and No detections (11.5%) is 3.9σ. For this setting, the fraction of Expected detections is 46.9%, with the remaining 32.3% resulting in Too Late detections. These percentages reasonably match the results obtained from the subjective button press data, for which we found 6.25% Too Early detections, 50.0% Expected detections, 42.7% Late detections and 1.05% No detections. For reference, when the DR-1 limits from (Phatak and Bekey, 1969b) are applied, which for this experiment corresponds to detection boundaries of 12σ for e and 6σ for $\dot{e}$, there would be no Too Early detections and no Expected detections, but 7.3% Late detections and 92.7% No detections. Overall, the proposed detection limits, based on 3.9 times the e and $\dot{e}$ standard deviations, seem to faithfully represent human operators' detection of changes in CE dynamics in our experiment. In future work, experiments with other CE transitions – e.g., matching those of earlier experiments by Phatak and Bekey (1969b) – should be performed to verify to what extent our proposed limits may be more generally applicable.

5. CONCLUSIONS

In this paper, we focused on predicting human operators' detection of a change in Controlled Element (CE) dynamics from variations in tracking error and error rate. For this research, a dedicated experiment with six skilled participants was performed, in which a tracking task was performed with a CE that transitioned from approximate single integrator to double integrator dynamics. The participants indicated, by pressing a trigger button on the side stick, when they detected a CE transition. Results show that human operators' detection of a CE change can be linked to occurring statistical 'outliers' in the error (e) or error rate ($\dot{e}$) signals, but that previously proposed detection limits (Phatak and Bekey, 1969b) ($2|\dot{e}_{max}|$, DR-1) are insufficiently sensitive to explain our experiment data. For our tested CE transition, operators detected a CE change after occurrences of e and $\dot{e}$ values outside of 2-6 times their respective pre-transition standard deviations. Based on this, new detection limits proportional to the pre-transition standard deviations of e and $\dot{e}$ were proposed and applied for predicting our measured detection data. The best detection limit was found to be 3.9σ, which resulted in a reasonable match with the measured subjective detections, with only 9.38% false positives (too early detections) and 11.5% false negatives (missed detections). Overall, our analysis suggests that human operator adaptation is likely triggered by statistical variations in tracking error and error rate, which may be used directly for developing predictive models of human adaptation.

REFERENCES

Hess, R.A. (2009). Modeling pilot control behavior with sudden changes in vehicle dynamics. *Journal of Aircraft*, 46(5), 1584–1592.

Miller, D.C. and Elkind, J.I. (1967). The adaptive response of the human controller to sudden changes in controlled process dynamics. *IEEE Trans. on Human Factors in Electronics*, HFE-8(3), 218–223.

Mulder, M., Pool, D.M., Abbink, D.A., Boer, E.R., Zaal, P.M.T., Drop, F.M., van der El, K., and van Paassen, M.M. (2018). Manual control cybernetics: State-of-the-art and current trends. *IEEE Trans. on Human-Machine Systems*, 48(5), 468–485.

Niemela, R.J. and Krendel, E.S. (1975). Detection of a change in plant dynamics in a man-machine system. *IEEE Trans. on Systems, Man, and Cybernetics*, SMC-5(6), 615–617.

Phatak, A.V. and Bekey, G.A. (1969a). Decision processes in the adaptive behavior of human controllers. *IEEE Trans. on Systems Science and Cyb.*, 5(4), 339–351.

Phatak, A.V. and Bekey, G.A. (1969b). Model of the adaptive behavior of the human operator in response to a sudden change in the control situation. *IEEE Trans. on Man-Machine Systems*, 10(3), 72–80.

Phatak, A.V. (1969). *On the adaptive behavior of the human operator in response to a sudden change in the control situation.* Ph.D. thesis, Univ. of S. California.

Plaetinck, W., Pool, D.M., van Paassen, M.M., and Mulder, M. (2019). Online identification of pilot adaptation to sudden degradations in vehicle stability. *IFAC-PapersOnLine*, 51(34), 347–352.

Thorpe, S., Fize, D., and Marlot, C. (1996). Speed of processing in the human visual system. *Nature*, 381(6582), 520–522.

Weir, D.H. and Phatak, A.V. (1967). Model of human operator response to step transitions in controlled element dynamics. NASA Contractor Report CR-671.

Young, L.R. (1969). On adaptive manual control. *Ergonomics*, 10(4), 292–331.

Young, L.R., Green, D.M., Elkind, J.I., and Kelly, J.A. (1964). Adaptive dynamic response characteristics of the human operator in simple manual control. *IEEE Trans. on Human Factors in Electronics*, HFE-5(1).

Zaal, P.M.T. (2016). Manual control adaptation to changing vehicle dynamics in roll–pitch control tasks. *Journal of Guidance, Control, and Dynamics*, 39(5), 1046–1058.